

High-pressure induced phase transitions of Y_2O_3 and $Y_2O_3:Eu^{3+}$

Lin Wang,^{1,a)} Yuexiao Pan,² Yang Ding,¹ Wenge Yang,³ Wendy L. Mao,^{4,5,a)} Stanislav V. Sinogeikin,³ Yue Meng,³ Guoyin Shen,^{1,3} and Ho-kwang Mao^{1,3,6}

¹HPSynC, Carnegie Institution of Washington, 9700 South Cass Avenue, Argonne, Illinois 60439, USA

²College of Chemistry, South China University of Technology, Guangzhou 510641, People's Republic of China

³HPCAT, Carnegie Institution of Washington, 9700 South Cass Avenue, Argonne, Illinois 60439, USA

⁴Geological and Environmental Sciences, Stanford University, 450 Serra Mall, Stanford, California 94305-2115, USA

⁵Photon Science, Stanford Linear Accelerator Center, 2575 Sand Hill Road, Menlo Park, California 94025, USA

⁶Geophysical Laboratory, Carnegie Institution of Washington, 5251 Broad Branch Road NW, Washington, DC 20015, USA

(Received 13 October 2008; accepted 21 January 2009; published online 13 February 2009)

We investigated high-pressure induced phase transitions in Y_2O_3 and Eu-doped Y_2O_3 ($Y_2O:Eu^{3+}$) using angular dispersive synchrotron x-ray diffraction, Raman spectroscopy, and photoluminescence (PL). With increasing pressure, we observed a series of phase transformations in $Y_2O_3:Eu^{3+}$, which followed a structure sequence of cubic \rightarrow monoclinic \rightarrow hexagonal, while Y_2O_3 followed a sequence of cubic \rightarrow hexagonal. During decompression, both hexagonal structured Y_2O_3 and $Y_2O_3:Eu^{3+}$ transformed into monoclinic phases which were quenchable back to ambient pressure. Raman and PL measurements shed additional light on the different phase transition behavior in these two samples. © 2009 American Institute of Physics. [DOI: 10.1063/1.3082082]

Pressure induced phase transitions in oxides with d and f electrons have generated increasing interest since pressure provides a unique way to study the structure stability affected by the coupling between charge, spin, orbital, and lattice.¹ For example, phase transitions in lanthanide sesquioxides (Ln_2O_3) have been an attractive area.^{2,3} The first systematic investigation was reported over 80 years ago and the original proposed three phase diagram (denoted as phases A, B, and C) is still in use.⁴ Phases A, B, and C have hexagonal, monoclinic, and cubic structures, respectively. At ambient conditions, the sequence of density for the phases of Ln_2O_3 is $\rho_A > \rho_B > \rho_C$ so with increasing pressure, it is expected that structure transitions will follow the sequence $C \rightarrow B \rightarrow A$ for Ln_2O_3 ,⁵ an expectation which has been supported by experimental results.^{3,6}

Yttria (Y_2O_3) is a rare earth sesquioxide which has been widely used in coating materials and as a red-emitting phosphor.^{7,8} Since the electronegativity and ionic radius of yttrium are very close to lanthanide elements, it is believed that Y_2O_3 should display similar crystal structure and transition behavior as Ln_2O_3 .^{9–11}

High-pressure induced phase transitions of Y_2O_3 have previously been studied using x-ray diffraction (XRD) and Raman spectroscopy.^{11–13} However, the phase transformations in Y_2O_3 from previous reports have been inconsistent. Atou *et al.*¹² studied the shock-induced phase transition in Y_2O_3 . Their results indicated that C-type structured Y_2O_3 transformed to B-type above 12 GPa and completed of this transition at 20 GPa. They did not observe the predicated transition from B-type to A-type over the pressure range studied. Ma *et al.*¹³ reported two structural transitions in Y_2O_3 . A transition from C-type to B-type began at 12.8 GPa and then the B-type transformed to a new phase at 21.8 GPa.

However, the structure of the new phase was not determined. Husson *et al.*¹¹ studied the *in situ* high-pressure Raman spectra of Y_2O_3 to 22 GPa. They found that C-type Y_2O_3 transformed to B-type at 12 GPa and the B-type then transformed to A-type at 19 GPa.

Another interesting problem to be investigated is how the very small amounts of dopants affect structure stability at high pressure. In our study, we investigated Eu^{3+} doped Y_2O_3 ($Y_2O_3:Eu^{3+}$) which has attracted a great deal of attention as the main red-emitting material in fluorescent lamps and projection television tubes.¹⁴ It was found that the luminescence from $f-f$ transitions in Eu^{3+} is very sensitive to the Eu^{3+} ion environment and can be used as a spectral probe to identify the crystal structure.¹⁵ Recently, Bai *et al.*¹⁵ studied the *in situ* high-pressure luminescence spectra of nanocrystalline and bulk $Y_2O_3:Eu^{3+}$. Their results indicated that the C-type bulk $Y_2O_3:Eu^{3+}$ transformed into the B-type at 15 GPa, while 20 nm-sized nanocrystals do not. However, the phase transition in $Y_2O_3:Eu^{3+}$ has not been studied by XRD which would give direct evidence on the nature of the structural changes.

We examined the phase transitions of Y_2O_3 and for the first time, we investigated $Y_2O_3:Eu^{3+}$ using *in situ* angular dispersive synchrotron x-ray diffraction (ADXRD), Raman spectroscopy, and photoluminescence (PL) measurements under high pressure. We observed that the phase transitions in $Y_2O_3:Eu^{3+}$ followed a $C \rightarrow B \rightarrow A$ sequence while Y_2O_3 followed a $C \rightarrow A$ sequence. The Raman and PL studies showed that the lattice vibration and electron states were changed due to the doping of Eu^{3+} into the Y_2O_3 , which provided clues for understanding the differences between the two samples.

A Mao-type diamond anvil cell was used to generate pressure in the sample. Samples were loaded into $\sim 100 \mu\text{m}$ diameter holes drilled in T301 stainless steel gaskets. Silicone oil was used as a pressure-transmitting medium. Pres-

^{a)}Authors to whom correspondence should be addressed. Electronic addresses: wanglin@aps.anl.gov and wmao@stanford.edu.

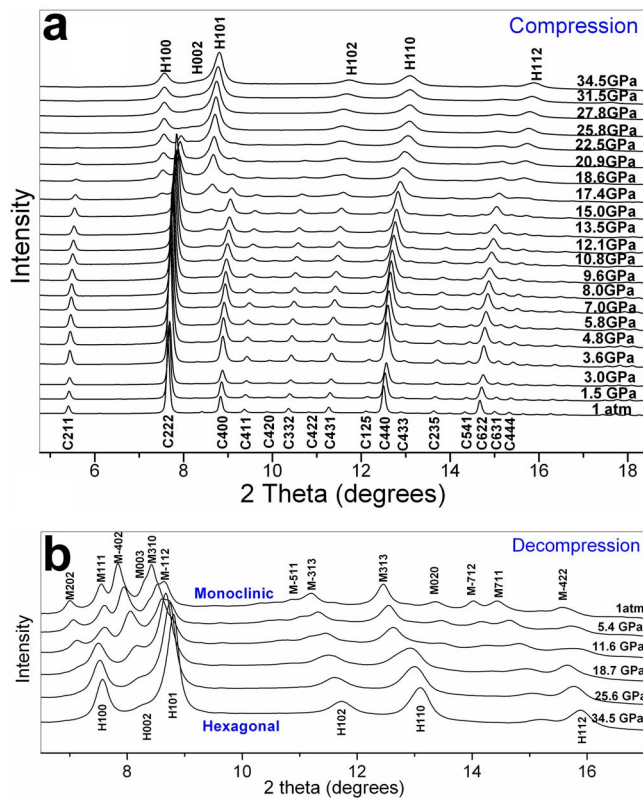


FIG. 1. (Color online) XRD patterns for Y_2O_3 upon compression (a) and decompression (b) $\lambda=0.4084(1)$ Å.

sure was determined from the fluorescence spectra of the ruby.¹⁶ The *in situ* high-pressure ADXD experiments were carried out at 16ID-B station of the Advanced Photon Source, Argonne National Laboratory. A focused monochromatic beam [$\lambda=0.4084(1)$ Å] of approximately 5 μm in diameter was used for the ADXD measurements.

Typical high-pressure XRD patterns collected from Y_2O_3 are shown in Fig. 1(a). At an ambient pressure, the structure was cubic (C-type, $Ia3$) with $a=10.603$ Å which is in agreement with previous measurements.¹³ During compression, no changes were observed below 12.1 GPa, indicating that the sample remained as C-type. Above 12.1 GPa, new peaks at 2θ of 7.5° , 8.6° , 11.4° , and 15.7° appeared which could be indexed with hexagonal symmetry (A-type). The intensities of the new peaks increased with increasing pressure as the A-type grew at the expense of the C-type with complete conversion at 22.5 GPa. The A-type structure remained stable to 34.5 GPa which was the highest pressure of the experiment. Figure 1(b) shows the XRD patterns of Y_2O_3 of different pressures during decompression. The A-type was not quenchable and transformed to another phase which was indexed as B-type.

Our experiments showed that the pressure transition scenario of Y_2O_3 is $C \rightarrow A$ instead of $C \rightarrow B \rightarrow A$ and that during decompression, the phase transition sequence is $A \rightarrow B$. The B-type structure can be preserved to ambient pressure. This result differs from previous XRD studies. It is not surprising that the study on samples quenched from high pressures did not observe the A-type phase since we found that it is not quenchable which speaks to the importance of *in situ* characterization.¹² In comparison with the results of the previous *in situ* Raman and EDXD studies,¹³ we did not observe the phase transition of $C \rightarrow B$ reported by Husson *et al.*¹¹ and

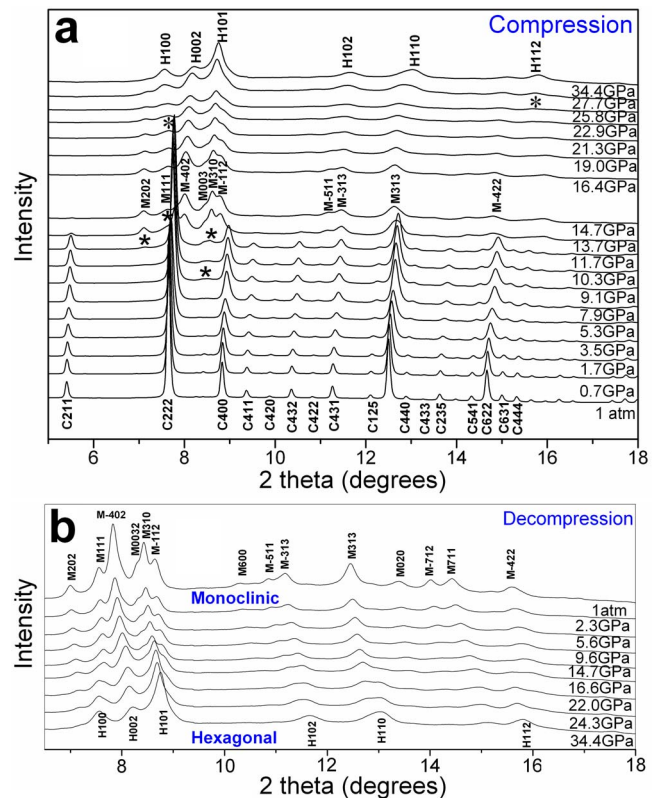


FIG. 2. (Color online) XRD patterns for $Y_2O_3:Eu^{3+}$ during compression (a) and decompression (b) $\lambda=0.4084(1)$ Å. Asterisks mark the first appearance of new peaks due to the A-type.

Ma *et al.*,¹³ even though the highest pressure in our experiment was higher than in previous studies. Note that the phase transition route in our high-pressure experiments is consistent with the thermal phase diagram of Y_2O_3 in which the cubic phase of Y_2O_3 is stable up to 2325 °C and it is transformed into hexagonal phase at higher temperature.¹⁷ In addition, a similar phase transition route has been found in *in situ* XRD studies of other rare earth sesquioxides, Sm_2O_3 , Eu_2O_3 , and Gd_2O_3 ,^{5,18,19} which supports our finding.

We further studied the high-pressure induced phase transition of $Y_2O_3:Eu^{3+}$ (molar ratio $Y^{3+}:Eu^{3+}=99:1$). Figure 2(a) shows the high pressure XRD patterns for $Y_2O_3:Eu^{3+}$. At ambient pressure, $Y_2O_3:Eu^{3+}$ is in a cubic structure (C-type, $Ia3$) with $a=10.608$ Å, the same structure as pure Y_2O_3 . During compression, sample the remained in C-type structure below 7.9 GPa before new peaks were observed. The new peaks can be indexed with a monoclinic symmetry (B-type). The intensity of these new peaks increased as pressure increased, while the peak intensity of C-type structure decreased and disappeared completely at 14.7 GPa.

Figure 2(a) also shows the XRD spectra of $Y_2O_3:Eu^{3+}$ at higher pressures. It is found that the B-type remained stable up to about 19 GPa, and then the intensity of some diffraction peaks of the B-type became weaker. Gradually, some new peaks appeared at 25.8 GPa. The new peaks can be indexed with hexagonal symmetry (A-type). Above 27.7 GPa, the diffraction peaks of B-type disappeared, and the sample transformed into A-type structure completely. The A-type structure was stable up to 34.4 GPa, the highest pressure of the experiment.

Figure 2(b) shows the XRD patterns of $Y_2O_3:Eu^{3+}$ during decompression. It was found that the A-type structure

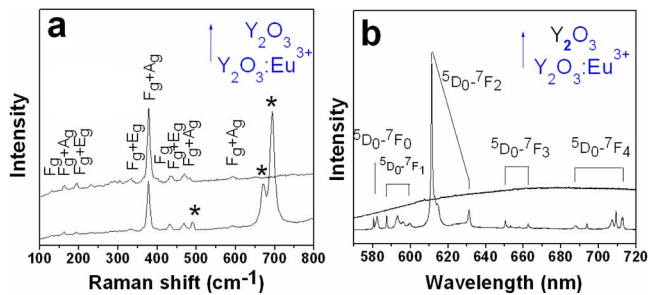


FIG. 3. (Color online) (a) Raman and (b) PL spectra of Y₂O₃ and Y₂O₃:Eu³⁺ excited by a 514.5 nm laser.

was not quenchable and it transformed into *B*-type during the decompression. The phase transition from *B*-type to *A*-type is reversible. The *A*-type phase transformed into *B*-type during the decompression and the *B*-type structure can be recovered to ambient pressure. However, the phase transition from *C*-type to *B*-type is irreversible.

Comparison with Y₂O₃, not only finds that the pressure of the phase transitions are different but also the phase transitions routes are different. From the data, *C*-type structural Y₂O₃ transformed into *A*-type directly at the pressure of 12.1 GPa and the *A*-type structure kept stable up to the highest pressure of the experiment. However, the *C*-type structural 1% Eu³⁺ doped Y₂O₃ transformed into *B*-type but not the *A*-type structure. The pressure of the phase transition is 7.9 GPa which is about 4.2 GPa lower than the pressure of the phase transition of pure Y₂O₃. The *B*-type structural Y₂O₃:Eu³⁺ transformed into *A*-type structure at 25.8 GPa. The two samples have same crystal structures and similar lattice parameters, and differ only in the 1% Eu³⁺ doping. To understand how the 1% Eu³⁺ doping changed the structure stability compared with pure Y₂O₃, we studied the lattice vibrations and electronic states of the two samples by measuring the Raman spectra and PL, respectively. Figure 3 shows the Raman and PL spectra of the samples excited by Ar⁺ ion laser with a wavelength of 514.5 nm. Compared to Y₂O₃, some new Raman peaks marked were observed in the Raman spectrum of Y₂O₃:Eu³⁺. Furthermore, the intensity of some of the peaks was lower than those of pure Y₂O₃. All of these changes indicate that the lattice vibrations were changed by doping, although no difference of the crystal structure was observed by comparison of the XRD patterns.

As shown in the figure, the PL spectra of the two samples were dissimilar. No PL peaks can be recognized from the spectrum measured from pure Y₂O₃. However, Y₂O₃:Eu³⁺ shows a very strong PL. This indicates that the electron states of the two samples are different. From previous studies, the main peak at around 612 nm was assigned to the ⁵D₀→⁷F₂ transition in C₂ symmetry for Eu³⁺ incorporated in Y₂O₃.^{8,20} The peaks at 582 and 587 nm of Y₂O₃:Eu³⁺ were assigned to the ⁵D₀→⁷F_{1a} transition of Eu³⁺ in S₆ and C₂ symmetries, respectively. Thus, the Eu³⁺ ions occupy both Y³⁺ sites in the lattice. As we know, the diameter of Eu³⁺ is 0.95 Å which is about 6% bigger than Y³⁺ (0.89 Å). Therefore, the crystal field strength of the oxygen coordination is increased due to the presence of rela-

tively larger cations in the lattice of Y₂O₃. The crystal field strength, the lattice vibrations, and electron states were changed due to the doping of Eu³⁺ into the Y₂O₃ which provide an insight into the difference in the pressure induced phase transitions caused by the doping.

In summary, we studied the pressure induced phase transition of pure and Eu³⁺ doped Y₂O₃. The results show that for pure Y₂O₃ during compression, the *C*-type structure transformed into *A*-type at 12.1 GPa and *A*-type structure kept stable up to 34.5 GPa, and under decompression the *A*-type structure transformed into *B*-type and *B*-type can be recovered to ambient pressure. For 1% doped Y₂O₃:Eu³⁺ during compression, the *C*-type structure transformed into *B*-type at 7.9 GPa and *B*-type transformed further into *A*-type at the pressure of 25.8 GPa, and *A*-type kept stable at the pressure up to 34.4 GPa and during decompression, *A*-type transformed into *B*-type and *B*-type can be recovered to ambient pressure which is the same as pure Y₂O₃. Raman and PL studies confirmed that the lattice vibration and electron states were modified due to the presence of relatively bigger ion Eu³⁺ in the lattice of Y₂O₃, which provides an insight toward understanding the difference in the pressure induced phase transition properties between these two materials.

Use of the HPCAT facility was supported by DOE-BES, DOE-NNSA, NSF, and the W. M. Keck Foundation. Use of the Advanced Photon Source and Center for Nanoscale Materials were supported by the U. S. Department of Energy, Office of Science, Office of Basic Energy Sciences, under Contract No. DE-AC02-06CH11357.

- ¹Y. Ding, D. Haskel, S. G. Ovchinnikov, Y. C. Tsen, Y. S. Orlov, J. C. Lang, and H. K. Mao, *Phys. Rev. Lett.* **100**, 045508 (2008).
- ²H. R. Hoekstra and K. A. Gingerich, *Science* **146**, 1163 (1964).
- ³C. Meyer, J. P. Sanchez, J. Thomasson, and J. P. Itie, *Phys. Rev. B* **51**, 12187 (1995).
- ⁴V. M. Goldschmidt, F. Ulrich, and T. Barth, *Skr. Nor. Vidensk.-Akad., [Kl.] 1: Mat.-Naturvidensk. Kl.* **1925**, 5.
- ⁵Q. X. Guo, Y. S. Zhao, C. Jiang, W. L. Mao, and Z. W. Wang, *Solid State Commun.* **145**, 250 (2008).
- ⁶Q. X. Guo, Y. S. Zhao, C. Jiang, W. L. Mao, Z. W. Wang, J. Z. Zhang, and Y. J. Wang, *Inorg. Chem.* **46**, 6164 (2007).
- ⁷C. B. Willingham, J. M. Wahl, P. K. Hogan, L. C. Kupferberg, T. Y. Wong, and A. M. De, *Proc. SPIE* **5078**, 179 (2003).
- ⁸T. Igarashi, M. Ihara, T. Kusunoki, K. Ohno, T. Isobe, and M. Senna, *Appl. Phys. Lett.* **76**, 1549 (2000).
- ⁹L. Pauling and D. M. Sappel, *Z. Kristallogr.* **75**, 128 (1930).
- ¹⁰A. Fert, *Bull. Soc. Fr. Mineral. Cristallogr.* **89**, 194 (1966).
- ¹¹E. Husson, C. Proust, P. Gillet, and J. P. Itie, *Mater. Res. Bull.* **34**, 2085 (1999).
- ¹²T. Atou, K. Kusaba, K. Fukuoka, M. Kikuchi, and Y. Syono, *J. Solid State Chem.* **89**, 378 (1990).
- ¹³Y. M. Ma, H. A. Ma, Y. W. Pan, Q. L. Cui, B. B. Liu, T. Cui, G. T. Zou, J. Liu, and L. J. Wang, *Nucl. Technol.* **25**, 841 (2002).
- ¹⁴H. Z. Wang, M. Uehara, H. Nakamura, M. Miyazaki, and H. Maeda, *Adv. Mater. (Weinheim, Ger.)* **17**, 2506 (2005).
- ¹⁵X. Bai, H. W. Song, B. B. Liu, Y. Y. Hou, G. H. Pan, and X. G. Ren, *J. Nanosci. Nanotechnol.* **8**, 1404 (2008).
- ¹⁶H. K. Mao, J. A. Xu, and P. M. Bell, *J. Geophys. Res.* **91**, 4673 (1986).
- ¹⁷O. N. Carlson, *Bull. Alloy Phase Diagrams* **11**, 61 (1990).
- ¹⁸D. Lonappan, N. V. C. Shekar, P. C. Sahu, B. V. Kumarasamy, A. K. Bandyopadhyay, and M. Rajagopalan, *Philos. Mag. Lett.* **88**, 473 (2008).
- ¹⁹L. Wang, Y. Ding, W. G. Yang, and H. K. Mao (unpublished).
- ²⁰N. Chang and J. Gruber, *J. Chem. Phys.* **41**, 3227 (1964).